Distributed Event-triggered Control for Frequency Restoration in Islanded Microgrids with Reduced Trigger Condition Checking

Yulin Chen, *Member*, *IEEE*, Donglian Qi, *Senior Member*, *IEEE*, Zhenming Li, Zhenyu Wang, Xinyi Yang, and Jianliang Zhang

***Abstract*—For islanded microgrids (MGs), distributed control is regarded as a preferred alternative to centralized control for the frequency restoration of MGs. However, distributed control with successive communication restricts the efficiency and resilience of the control system. To address this issue, this paper proposes a distributed event-triggered control strategy for the frequency secondary control in islanded MGs. The proposed event-triggered control is Zeno behavior free and enables each DG to update and propagate its state to neighboring DGs only when a specific "event" occurs, which significantly reduces the communication burden. Compared with the existing event-triggered control, a trigger condition checking period of the proposed event-triggered control is provided to reduce the computation burden when checking the trigger condition. Furthermore, using the aperiodicity and intermittent properties of the communication, a simple detection principle is proposed to detect and isolate the compromised communication links in a timely and economic fashion, which improves the resilience of the system against FDI attacks. Finally, the control effectiveness of the proposed control scheme is validated by the simulation results of the tests on an MG with 4 DGs.**

***Index Terms*—Distributed control, event-triggered control, islanded microgrid, secondary control.**

I. Introduction

DUE to DGs' potential of improving energy efficiency, reliability, and sustainability [1], future power grids will be able to accommodate a large number of distributed generators (DGs). To better manage the integrated DGs, microgrid (MG) needs to play a vital role. An MG with appreciated control can operate in both grid-connected mode and islanded mode. Since a large number of advanced communicating and computing devices are deployed in MGs for better monitoring and controlling the systems, the MG becomes into a typical cyber-physical system with deep interaction of electric systems and communication networks [2].

Manuscript received November 3, 2020; revised February 15, 2021; accepted May 21, 2021. Date of online publication May 6, 2022; date of current version November 16, 2023. This work was supported by the National Key Research and Development Program of China (Basic Research Class) (2017YFB0903000) and the National Natural Science Foundation of China (U1909201).

Y. L. Chen, D. L. Qi (corresponding author, email: qidl@zju.edu.cn), Z. M. Li, Z. Y. Wang, X. Y. Yang and J. L. Zhang are with the College of Electrical Engineering, Zhejiang University, Hangzhou 310027, China.

DOI: 10.17775/CSEEJPES.2020.05730

For the control structure of MGs, hierarchical control is considered as a common control framework [3], [4], which includes primary, secondary and tertiary control levels. The primary control usually uses a droop mechanism to achieve autonomous power sharing only relying on measurements at the local states. The main tasks of the secondary control are to compensate for the deviation of frequency/voltage caused by the primary droop control and, additionally, to achieve desired power allocation [5]–[8]. The tertiary control is concerned more about the economy and optimality of the MGs' operations.

In islanded MGs, the main objective is to maintain a continuous power supply and keep the system stable. Thus, the tertiary control level appears to be not so important for islanded MGs, and what counts is the primary and secondary control levels. The secondary control is of great importance for the islanded MGs working at nominal conditions, keeping the system stable and increasing the quality of the power supply. Thus, the reliability of the secondary control is crucial [9]. Traditionally, the secondary control is governed by a centralized controller, which needs to collect global information from all the participating DGs and send the decision signals back to them. However, with an increasing number of DGs being accommodated, the centralized control would require the central master controller to have strong computing capability and the communication links should have sufficiently large bandwidth. In addition, any changes in communication topology or plug-and-play of the DGs and loads will cause changes in the control protocol. To this end, the distributed control strategies are developed and implemented in the MGs' operation and regulation due to their flexibility, scalability and better computational performance [9]–[13], especially at the secondary control level. With distributed control, each DG only needs its local and neighboring DGs' information through a sparse communication network to achieve the secondary control objective, which will reduce the infrastructure cost and improve the scalability. However, the existing distributed secondary control strategies are always based on successive communication and computation assumptions, because continuous control is usually implemented by a digital control system in practice applications, which means that the controller computes its protocol and propagates its decision in between an extremely small sampling period. Such an assumption requires DGs to have fast computation ability and the system

should have an ideal communication environment, which is obviously unrealistic for the DGs with limited computation ability [8]. In addition, the limited communication bandwidth could lead to traffic congestion when the system is scaling up. In such circumstances, designing an appreciated secondary control scheme should not only consider the achievement of desired control performance, but also consider the conservation of communication and computation resources.

In fact, the distributed secondary controllers do not necessitate successively operating, rather, they can be triggered only when some specified event occurs. In this sense, the distributed event-triggered control methods are developed to achieve the secondary control goals while reducing the communication burden [14]–[17]. The event-triggered controller does not require DGs to communicate with others and update their states successively, but only when required. Thus, the communication requirement is significantly reduced in this way. Furthermore, the aperiodic and intermittent way of date exchange among DGs would make the event-triggered controller have inherent ability to detect the successive false date injection (FDI) attacks on communication links, which will increase the resilience of the system. The main tasks for designing a distributed event-triggered control are twofold: one is to design a proper trigger condition that enables the convergence of the control system, the other is to prove that the designed controller does not exist with Zeno behavior (the controller updates and communicates an infinite number of times in a finite period [17]). So far, several distributed event-triggered control strategies for the secondary control in MGs have been investigated in literature [8], [18]–[21]. [8] introduces a distributed event-triggered method for frequency/voltage regulation and accurate real/reactive power sharing in islanded MGs. The two objectives are decoupled into two timescales, and the event-triggered distributed average consensus in [15] are used to design the event-triggered controllers only for power sharing control with a slower timescale, then the communication requirement is significantly reduced and the two objectives are achieved. [18] develops a proportional-integral-based secondary control, the authors provide a distributed triggering condition for each of the DGs to reduce the communication burden. The authors in [19] propose an instantaneous event-triggered secondary control strategy. In this study, a PI-free controller is designed to instantaneously compensate the frequency deviation, and an event-triggering mechanism is introduced to reduce the amount of communications in both transient and steady-state periods. In [20], a distributed dynamic event-triggered control scheme is proposed to deal with frequency restoration and active power sharing in MGs, which measurably reduces the communication burden. In addition, the varying communication time delays for the controller are investigated, and an upper bound of time delays is provided. A distributed event-triggered mechanism for dynamic average consensus to achieve fair current sharing and average DC voltage regulation in a DC microgrid is proposed in [21].

However, most of the existing distributed event-triggered secondary control of MGs requires each DG to successively evaluate its trigger condition with the sampling period of the digital control systems. However, the successive trigger condition checking requires each DG to mandate better computational ability than that of the traditional distributed secondary control, which increases the computation burden of each DG, even though it reduces the communication burden. Therefore, this paper proposes a novel event-triggered leader-follower tracking control for the frequency restoration of MGs with reduces trigger condition checking. In addition, a simple detection principle based on the aperiodic and intermittent communication of the proposed event triggered control is proposed to detect and isolate the compromised communication links in a timely and economical fashion. The contributions of this paper are as follows: 1) A novel distributed event-triggered control strategy for frequency restoration is proposed by designing a proper trigger condition without Zeno behavior, which significantly reduces the communication requirements in both transient and steady-state stages while achieving the control goal. 2) An upper bound of trigger condition checking periods, which can be dispersedly obtained by each DG, is provided to help each DG reduce the frequency of trigger condition checking, thereby reducing the computation burden. 3) A successive FDI attack detection and isolation method is proposed to identify and eliminate the attacks on communication links between each DG, which increases the resilience of the system.

The remainder of the paper is organized as follows. Section II introduces the traditional distributed secondary control for MGs and provides the problem statement. Section III shows the main results of this paper, in which a novel event-triggered condition of leader-follower tracking based secondary frequency control is developed, its Zeno behavior freeness is proved. Based on the proposed event-triggered controller, a trigger condition checking period is derived, and an FDI attack detection and isolation mechanism is provided. Section IV conducts some case studies to validate the proposed controller with a delicately simulated test MG. Finally, Section V presents the conclusion of this paper.

II. Distributed Secondary Control of MGs and Problem Statement

MG is a typical cyber-physical system, since it is a system including an electric network and a communication network, while the measuring and controlling implementations establish the interaction between the physical and cyber spaces. For the distributed secondary control in islanded MGs, only a sparse communication network is required, in which each DG only uses the local states and the states of its neighbors to cooperatively achieve the operational objective. The distributed secondary control framework of an MG with multiple DGs is shown in Fig. 1.

A. Communication Network

For an islanded MG with n DGs, the communication network can be modeled by a undirected graph $\boldsymbol{G} = (\boldsymbol{V}, \boldsymbol{E}, \boldsymbol{A})$, in which $\boldsymbol{V} = \{v_1, v_2, \cdots, v_n\}$ is the set of DGs, $\boldsymbol{E} \subset \boldsymbol{V} \times \boldsymbol{V}$ is the set of edges representing the communication links between DGs, and $\boldsymbol{A} = [a_{ij}]_{n\times n}$ is the adjacency matrix with

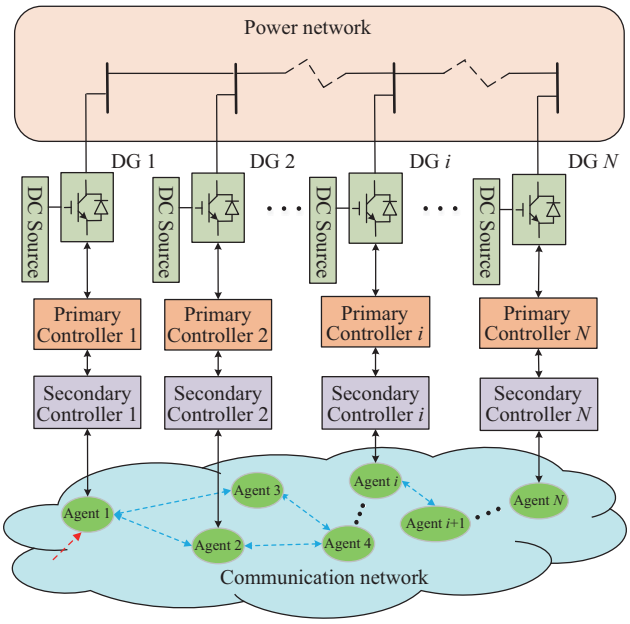

Fig. 1. The distributed secondary control framework of a MG with multiple DGs.

$a_{ii} = 0$ ($\forall i = 1, \cdots, n$), $a_{ij} = 1$ if DG j is the neighbor of DG i, i.e., $(v_i, v_j) \in \boldsymbol{E}$, and $a_{ij} = 0$ otherwise. Notice that, for an undirected graph, $a_{ij} = 1$ implies $a_{ji} = 1$, i.e., $A = A^{\mathrm{T}}$, where A^{T} is the transpose of $\boldsymbol{A}$. All the neighbors of DG i is denoted by $M_i = \{j | (v_i, v_j) \in \boldsymbol{E}\}$. The degree of the graph is stated as $\boldsymbol{D} = \mathrm{diag}\{d_1, \cdots, d_n\}$, where $d_i = \sum_{j=1}^{n} a_{ij}$. Then, the Laplacian matrix of graph G is defined as $\boldsymbol{L} = \boldsymbol{D} - \boldsymbol{A}$ [22]. A path in the graph G is a sequence of connected edges, and the graph is connected if there exists a path between every two DGs. In the sense that graph G is connected, the Laplacian matrix L is positive-semidefinite (i.e., the eigenvalues are non-negative) and irreducible. Assume that only several DGs (not all) can receive the reference value. Thus, a pinning matrix is defined by $\boldsymbol{B} = \mathrm{diag}\{b_1, \cdots, b_n\}$, where $b_i = 1$ implies that the pinned DG i can obtain the reference value, and $b_i = 0$ otherwise. Then, we define $\boldsymbol{H} = \boldsymbol{L} + \boldsymbol{B}$ [23].

B. Traditional Distributed Secondary Control

A DG is modeled as a voltage-controlled voltage source inverter in this paper. In the primary control layer, the decentralized droop control of each DG that emulates the behavior of the traditional synchronous generator can provide automatic power sharing. The typical droop mechanism of active power and frequency for DG i ($i = 1, \cdots, n$) is stated as follows [3], [4], [10]:

$$\omega_i = \omega_i^{\mathrm{set}} - K_i^P P_i \tag{1}$$

where ω_i is the angular frequency that can be converted into a frequency by $f_i = \omega_i / 2\pi$ Hz, ω_i^{set} is the nominal set-point of the angular frequency, K_i^P is the droop coefficient, and P_i is the active power of DG i's terminal.

The primary control layer also includes several inner control loops, i.e., the voltage, current, and power control loops [24]. The response speed of these control loops is faster than that of the droop control and any other high-level control, thus they can be neglected when studying the secondary control [3], [4].

Although the droop control allows the DGs to automatically share active power, it will cause frequency deviation in islanded MGs. Therefore, it requires the secondary control to restore the frequency deviation back to its reference value. To use the distributed control strategy in the secondary control of MGs, differentiating (1) yields:

$$\dot{\omega}_i = \dot{\omega}_i^{\mathrm{set}} - K_i^P \dot{P}_i \tag{2}$$

Accordingly, the set-point of the frequency for DG i is adjusted by the distributed secondary control as follows:

$$\omega_i^{\mathrm{set}} = \int \left(\dot{\omega}_i - K_i^P \dot{P}_i \right) \mathrm{d}t = \int \left(k_\omega u_i^\omega - K_i^P \dot{P}_i \right) \mathrm{d}t \tag{3}$$

where u_i^ω is the distributed secondary input, which is stated in (4), and $\dot{P}$ can be obtained from the power control loop [9].

$$u_i^\omega = -\sum_{j \in M_i} a_{ij}(\omega_i - \omega_j) - b_i(\omega_i - \omega_{\mathrm{ref}}) \tag{4}$$

where ω_{ref} is the reference frequency of the secondary control, which is usually set to be 50 Hz for islanded MGs.

It can be seen from the control law that the distributed secondary control only requires each DG to use the information of the local and from its neighbors to coordinately achieve the secondary control objective.

C. The Objective of Distributed Event-triggered Secondary Control

Notice that the traditional distributed secondary controller of each DG needs to successively get access to the information from its neighboring DGs to update the control signal in theory, which is a waste of both communication and control sources, and it would also increase the communication and computation burden when the system is scaling up. In fact, the communication and control signal update can be implemented discontinuously, i.e., the controller is triggered only when necessary. Thus, distributed secondary control can be achieved by event-triggered mechanisms. However, most of the existing event-triggered control strategy needs each agent to successively evaluate trigger conditions, which will in turn increase the computation burden of each DG. Therefore, the main objective of this paper is to design a distributed event-triggered secondary control scheme for islanded MGs with less communication and computation cost to achieve the secondary frequency control objective, specifically, for $i = 1, 2, \cdots, N$

$$\lim_{t \to \infty} |\varepsilon_i| = 0 \quad \forall i \in \boldsymbol{V} \tag{5}$$

where N is the number of DGs in MG, and

$$\varepsilon_i = \omega_i - \omega_{\mathrm{ref}} \tag{6}$$

is defined as the tracking error.

III. Distributed Event-triggered Secondary Control Design

To reduce the communication and computation burden

while achieving the secondary frequency control objective for islanded MGs, a novel event-triggering mechanism based distributed secondary strategy is developed in this section. Then, an FDI attacks defense method is proposed based on the proposed event-triggered control strategy.

A. Event-triggered Controller

Different from the continuous controller in (4), the event-triggered based secondary controller of each DG uses the estimates of its local and neighboring DGs' states, rather than their true states, to make the control decision, which is designed as:

$$\begin{aligned} u_i^{\omega} &= -kz_i \\ z_i &= \sum_{j\in M_i}(\hat{\omega}_i-\hat{\omega}_j)+d_i(\hat{\omega}_i-\omega_{\mathrm{ref}}) \end{aligned} \tag{7}$$

where k is the control gain, $\hat{\omega}_i$ is the estimate of DG i's ($i=1,2,\cdots,n$) frequency. The estimate $\hat{\omega}_i$ updates according to the following rules:

$$\hat{\omega}_i(t)=\omega_i(t_k^i),\quad t\in[t_k^i,t_{k+1}^i) \tag{8}$$

where t_k^i is the kth trigger time, which will be elaborated in Section III B, for $k=0,1,2,\cdots$. Clearly, (8) implies that the controller of DG i updates its estimate $\hat{\omega}_i$ by using the true frequency at the trigger time t_k^i and broadcasts it out to its neighbors, and the controller of DG i maintains $\hat{\omega}_i$ in between the events $[t_k^i,t_{k+1}^i)$. Therefore, u_i is continuously piecewise in the sense that it only changes when the trigger condition of DG i is fulfilled, or its neighboring DGs' events occur, otherwise, u_i remains unchanged.

B. Distributed Trigger Condition

From the previous analysis, one may notice that deriving the trigger condition is the key to designing an event-triggered controller. In this section, the trigger condition is deduced in detail.

First, some identifications are needed to facilitate the subsequent analysis. The estimate error e_i that characterizes the mismatch between the estimate frequency and the true frequency of DG i is defined by:

$$e_i=\hat{\omega}_i-\omega_i,\quad i\in\boldsymbol{V},\quad t\in[t_k^i,t_{k+1}^i) \tag{9}$$

This error is obtained locally and enables DG i to know how far the estimate $\hat{\omega}_i$ is away from its real frequency ω_i. And e_i becomes 0 when the event occurs at t_k^i.

For the overall system, using the stacked form of (7):

$$\boldsymbol{z}=\boldsymbol{H}(\hat{\boldsymbol{\omega}}-\mathbf{1}_n\omega_{\mathrm{ref}}) \tag{10}$$

where $\mathbf{1}_n$ denotes a vector of ones, and the stacked form of (9):

$$\boldsymbol{e}=\hat{\boldsymbol{\omega}}-\boldsymbol{\omega} \tag{11}$$

combining with the tracking error defined in (6) yields:

$$\boldsymbol{\varepsilon}=\boldsymbol{H}^{-1}\boldsymbol{z}-\boldsymbol{e} \tag{12}$$

where $\boldsymbol{H}$ is a positive definite [24], $\boldsymbol{\varepsilon}=[\varepsilon_1,\cdots,\varepsilon_n]^{\mathrm{T}}\in\mathbb{R}^n$, $\boldsymbol{e}=[e_1,\cdots,e_n]^{\mathrm{T}}\in\mathbb{R}^n$, $\boldsymbol{z}=[z_1,\cdots,z_n]^{\mathrm{T}}\in\mathbb{R}^n$, where $\mathbb{R}$ is the set of real numbers.

From the tracking error of DG i (6) and the estimate error (11), we have:

$$\dot{\boldsymbol{\varepsilon}}=\dot{\boldsymbol{\omega}}=-k\boldsymbol{H}(\boldsymbol{\varepsilon}+\boldsymbol{e}) \tag{13}$$

To reduce the communication frequency of secondary control for DG i ($i=1,2,\cdots,n$), the trigger time t_k^i and the trigger condition are explicitly defined.

The trigger time t_k^i, at which DG i updates and broadcasts its estimate $\hat{\omega}_i$ based on (8), is defined as:

$$t_k^i\inf\{t>t_{k+1}^i|f_i(t)=0\},\quad i\in\boldsymbol{V} \tag{14}$$

where $f_i(\cdot)$ is the trigger function that is defined by:

$$f_i(e_i,z_i)=|e_i|-\frac{\sqrt{\sigma_i}}{\delta_m}|z_i| \tag{15}$$

where $0<\sigma_i<1$ provides the flexibility of the controller, δ_m denotes the minimum singular value of matrix $\boldsymbol{H}$.

C. Convergence Analysis

By using the trigger condition defined above, the main theorem of the proposed control strategy is provided.

Theorem 1. The control strategy designed in (7) with the update rule in (8) ensures the islanded MG achieves the control objective (5) asymptoticly in the sense that:

$$\omega_i\to\omega_{\mathrm{ref}}\quad as\quad t\to\infty,\ i\in V \tag{16}$$

while the DG i' controller only updates and broadcasts its estimate $\hat{\omega}_i$ at the trigger time defined in (14) and the trigger function defined in (15).

Proof: We evaluate the convergence of the proposed event-triggered control scheme by analyzing the evolution of the tracking error using the following Lyapunov function candidate $V:\mathbb{R}^n\to\mathbb{R}$ as:

$$V=\frac{1}{2}\boldsymbol{\varepsilon}^{\mathrm{T}}\boldsymbol{H}\boldsymbol{\varepsilon} \tag{17}$$

With (12) and (13), the derivative of (17) takes the form of:

$$\dot{V}=\boldsymbol{\varepsilon}^{\mathrm{T}}\boldsymbol{H}\dot{\boldsymbol{\varepsilon}}=-k\boldsymbol{z}^{\mathrm{T}}\boldsymbol{z}+k\boldsymbol{z}^{\mathrm{T}}\boldsymbol{H}\boldsymbol{e} \tag{18}$$

By using the Young's inequality $x^{\mathrm{T}}y\le\frac{\alpha}{2}\|x\|^2+\frac{1}{2\alpha}\|y\|^2$ with $\alpha>0$, since $\boldsymbol{H}$ is symmetric and positive definite, (18) can be upper bounded by:

$$\begin{aligned} \dot{V} &\le -k\|\boldsymbol{z}\|^2+k\delta_m\left(\frac{\alpha}{2}\|\boldsymbol{z}\|^2+\frac{\|\boldsymbol{e}\|^2}{2\alpha}\right) \\ &\le -k\sum_{i=1}^{n}\left[\left(1-\frac{\delta_m\alpha}{2}\right)|z_i|^2-\frac{\delta_m}{2\alpha}|e_i|^2\right] \end{aligned} \tag{19}$$

where δ_m represents the maximum singular value of matrix $\boldsymbol{H}$.

Let:

$$|e_i|^2=\frac{\sigma_i(2\alpha-\delta_m\alpha^2)}{\delta_m}|z_i|^2 \tag{20}$$

(19) can then be rewritten as:

$$\dot{V}\le -k\sum_{i=1}^{n}\left[(1-\sigma_i)\left(1-\frac{\delta_m\alpha}{2}\right)|z_i|^2\right] \tag{21}$$

By choosing $0 < \sigma_i < 1$ and $0 < \alpha < \frac{2}{\delta_m}$, V is strictly a negative definite.

Notice that function $f(\alpha) = 2\alpha - \delta_m \alpha^2$ has the maximum value $\max\{f(\alpha)\} = 1/\delta_m$ at $\alpha = 1/\delta_m$ in its definition domain of $(0, 2/\delta_m)$. Thus, each of DGs can use $\alpha = 1/\delta_m$ to obtain the optimal trigger condition $|e_i|^2 = \sigma_i |z_i|^2/\delta_m^2$. Then, (21) becomes:

$$\dot{V} \leq -k \sum_{i=1}^{n} \frac{1}{2}(1 - \sigma_i)|z_i|^2 \tag{22}$$

The proof is complete.

Remark 1. Notice that to evaluate the trigger condition, only the estimate error e_i, the control input z_i and the maximum singular value of matrix $\boldsymbol{H}$ δ_m are required for DG i. e_i and z_i are local signals, while δ_m can either be obtained dispersedly for DG i [24]–[28], or can be enforced previously by the designer. Thus, the proposed event-triggered controller is fully distributed.

Remark 2. Each event-trigger controller can decide when to trigger and propagate states to its neighbors based on the designed trigger function and the trigger condition, but not decide when to receive the information from its in neighbors, because the triggers are aperiodic and unpredictable. In other words, the data reception of each controller is passive.

An important observation is that, the following case may happen: a received estimate from a neighbor of DG i might lead to a discontinuity in the evaluation of $f(t)$, where just before the neighbor's estimate was received, $f(t) < 0$, while immediately after, $f(t) > 0$ [17]. Such a case would cause the controller to lose the trigger. Therefore, instead of updating and broadcasting the estimate only when $f(t) = 0$, the following definition of the trigger condition is preferred:

$$f_i(t) \geq 0 \tag{23}$$

To reduce the communication at the steady-state period, the following condition is also implemented,

$$\begin{cases} |\omega_{\text{ref}} - \hat{\omega}_i| \geq \gamma & \text{for } b_i = 1 \\ |z_i| \geq \gamma & \text{for } b_i = 0 \end{cases} \tag{24}$$

where γ is a threshold, which is a very small positive constant. (24) implies when the last estimate state is in a very small neighborhood of the reference value of the frequency, the controller does not cause a trigger any more.

The module diagram of the proposed event-triggered distributed secondary controller is illustrated in Fig. 2. Notice that the event-triggered controller is also located at each DG's location, and only uses its own and neighbors' states to execute the secondary control. However, different from the traditional controller, the event-triggered controller does not directly use the real states, rather it executes the following steps.

In each sampling period, for the controller of DG i, we have $(i = 1, 2, \cdots, n)$.

Step 1: Compute the trigger function with ω_i, $\hat{\omega}_i$ and z_i based on (15).

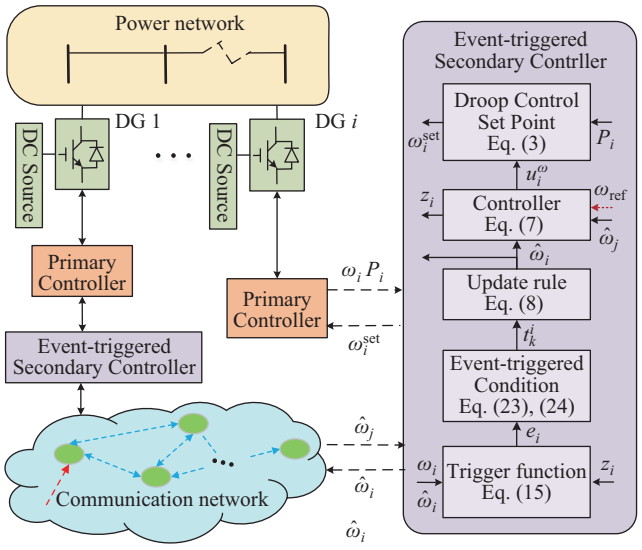

Fig. 2. The module diagram of the proposed event-triggered distributed secondary controller.

Step 2: Determine if the current time is the trigger time using the trigger condition defined in (23) & (24). If the trigger condition is satisfied, go to Step 3, otherwise, go to Step 4.

Step 3: Update $\hat{\omega}_i$ with the real frequency ω_i based on the update rule (8).

Step 4: Compute u_i^{ω} based on (7). Then, obtain the droop control set point ω_i^{set} using (3) and send it to the primary controller.

D. Zeno Behavior Freeness

Another important issue which needs to be considered for the event-triggered controller is its Zeno behavior, which refers to the fact that the events of a controller occur an infinite number of times in a finite period [17]. A well-designed event-triggered controller should avoid Zeno behavior. In this section, we will show that the proposed event-triggered mechanism is Zeno behavior free by deriving a positive lower bound for the intervals of two adjacent events. The following Lemma states our results.

Lemma 1. The proposed distributed event-triggered secondary frequency controller (7) does not exhibit Zeno behavior such that its minimum interval of two adjacent events $\tau \in \mathbb{R}_+$ is lower bounded by:

$$\tau \geq \frac{1}{k} \frac{\sqrt{\sigma_i}}{\delta_m} > 0 \tag{25}$$

Proof: To show not any DG's controller updates and broadcasts its estimate for an infinite number of times in a finite period, we examine the inter-event interval when DG i $(i = 1, 2, \cdots, n)$ does not obtain new estimates from its neighbors. Assume DG i's event just occurred at t_0, i.e., $e_i(t_0) = 0$. For $t \geq t_0$, while no new estimates are received from neighboring DGs, $\hat{\omega}_i$ and $\hat{\omega}_j$ they remain constant. Thus, one can derive from (9) that $\dot{e}_i = -\dot{\omega}_i$, and by integrating form t_0 to t

$$e_i(t) = k(t - t_0) z_i \tag{26}$$

Then, we try to find the next trigger time t^* when the trigger condition is fulfilled, i.e., $f_i(t^*) \geq 0$. If $z_i = 0$, no triggers will ever occur for $t \geq t_0$ since $e_i(t) = 0$, which means the control objective has been achieved. Thus, we consider the case when $z_i \neq 0$. After next trigger time $t^* \geq t_0$, by using (26) and the trigger condition defined in (23), we have:

$$k^2(t^* - t_0)^2 z_i^2 - \frac{\sigma_i}{\delta_m^2} z_i^2 \geq 0 \tag{27}$$

Therefore, the lower bound of the inter-event time is expressed by

$$\tau = t^* - t_0 \geq \frac{1}{k} \frac{\sqrt{\sigma_i}}{\delta_m} > 0 \tag{28}$$

The proof is complete.

E. Reduction of Trigger Condition Checking

Although the proposed distributed event-triggered controller can reduce the communication burden during both steady state and transient state, each of DGs needs to successively check its trigger condition with the sampling period of the control system, which significantly increases the computation burden of each DG. Therefore, in this section, a trigger condition checking period $h \in \mathbb{R}_+$ is provided to lengthen the period of trigger condition checking and reduce the computation burden. We use $\{t_n\}(t_{n+1} = t_n + h, n \in \{0, \mathbb{Z}_+\})$ to denote the sequence of times at which DGs check their trigger condition.

The following Lemma shows the sufficient condition for h.

Lemma 2. Each of the DGs only checks its trigger condition at t_n ($t_{n+1} = t_n + h$) with the trigger condition checking period h satisfying:

$$h < \frac{1 - \sigma_{\max}}{2k\delta_m} \tag{29}$$

Then, the controller designed in (7) with the update rule in (8) ensures the islanded MG achieves the control objective (5) asymptoticly.

Proof: Under the proposed event-triggered control with reduced trigger condition checking, the trigger condition (23) and (24) is only guaranteed at t_n. Thus, we analyze the defined Lyapunov function (17) in between t_n and t_{n+1}. For $t \in [t_n, t_n + h)$, integrating $\dot{e}_i = -\dot{\omega}_i$ from t_n to t, we have:

$$\boldsymbol{e}(t) = \boldsymbol{e}(t_n) + (t - t_n)k\boldsymbol{z}(t_n) \tag{30}$$

Substituting (30) in (18), we obtain:

$$\begin{aligned} \dot{V} = &-k\boldsymbol{z}^{\mathrm{T}}(t_n)\boldsymbol{z}(t_n) + k\boldsymbol{z}^{\mathrm{T}}(t_n)\boldsymbol{H}\boldsymbol{e}(t_n) \\ &+ k^2(t - t_n)\boldsymbol{z}^{\mathrm{T}}(t_n)\boldsymbol{H}\boldsymbol{z}(t_n) \end{aligned} \tag{31}$$

for all $t \in [t_n, t_n + h)$.

Then, using (22), we can derive from (31) that:

$$\begin{aligned} \dot{V} &\leq -k\sum_{i=1}^{n} \frac{1}{2}(1 - \sigma_i)|z_i(t_n)|^2 + k^2 h\delta_m \sum_{i=1}^{n} |z_i(t_n)|^2 \\ &= -k\sum_{i=1}^{n} \left[\frac{1}{2}(1 - \sigma_i) - kh\delta_m\right] |z_i(t_n)|^2 \end{aligned} \tag{32}$$

By choosing $h < \frac{1-\sigma_{\max}}{2k\delta_m}$, V is strictly a negative definite, which concludes the proof.

Note that the trigger condition checking period is determined by σ_i, k and δ_m. Since each DG knows its own σ_i, and k, δ_m can be obtained dispersedly by each DG, each DG can compute h dispersedly as well.

It is worth noting that the proposed distributed event-triggered control method can also be used in voltage restoration of islanded MGs, since the design of the distributed secondary voltage control law can be the same as that of the secondary frequency control, see [10]. However, due to space limitation, this paper only analyzes the frequency restoration of islanded MGs.

F. Detection of FDI Attacks on Communication Links

Although the distributed secondary control has the advantages of flexibility, scalability and better computation performance, the computation as well as the communication network expose the system to potential cyber-attacks, especially for the date exchange among DGs through communication links. The attacker can easily inject malicious signals into the communication links through the corresponding DGs' receivers or transmitters. For the secondary control of frequency restoration, the FDI attacks on the communication links between DG i and DG j can be modeled as [1], LOCALREF

$$u^{\delta} = -\sum_{j=1}^{n} a_{ij}(\omega_i - (\omega_j + \Delta_{ij})) - b_i(\omega_i - \omega_{\mathrm{ref}}) \tag{33}$$

where u^{δ} is the corrupted control input for the distributed secondary control, Δ_{ij} is the successive injection by the attackers, which can be unbounded.

The authors in [1] have illustrated that the FDI attacks on communication links will lead to tracking error ε_i which fails to converge to zero, that is:

$$\lim_{t\to\infty} \boldsymbol{\varepsilon}(t) > \boldsymbol{H}^{\mathrm{T}}|\boldsymbol{M}|\Delta_0 \geq 0 \tag{34}$$

where $\boldsymbol{M}$ denotes the communication incidence matrix, $\Delta_0 > 0$ is the lower bound of absolute value of the attack signal Δ_{ij}. This indicates that the communication links being injected by FDI attacks could result in the system frequency being out of synchronous, which would lead to other stability problems or even crash the overall system. Therefore, the detection and isolation of the attacks on communication links are of importance for the normal operation of MGs.

In traditional distributed secondary control, each DG executes (4) and propagates its updated states to its neighbors with the sampling period of the control system. The proposed event-triggered secondary controller of each DG also executes (7) with the sampling period of the control system, but dispite the traditional distributed secondary control, it exchanges dates with its neighbors aperiodically and intermittently. The data transmission (DT) is different. Therefore, if the attackers do not know the system is equipped with event-triggered controllers, they would inject malicious signals following the sampling period of the control system, i.e., the FDI attacks are successive with the same sampling period as the control system. The difference between communications of event-triggered control and successive FDI attacks is shown in Fig. 3.

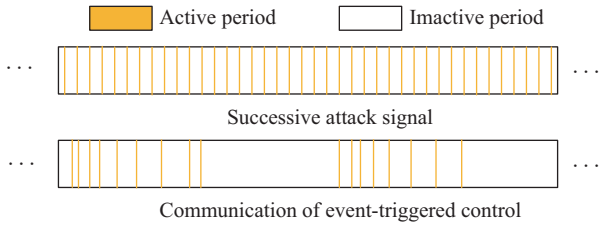

Fig. 3. The difference between communication of event-triggered control and successive FDI attack.

Therefore, inspired by the method in [1], by using the difference of DT between attack signals and event-triggered control signals, each DG can detect the successive FDI attacks by measuring the DT. If the DT frequency of any communication links is equal to the sampling frequency of the control system for a period of time, the communication link is identified as being attacked by malicious injections, then the related DGs discard these links, i.e., refuse to use the date from the corrupted link. Using this simple but effective principle, the proposed event-triggered controller can timely detect and isolate the corrupted communication links, while ensuring the achievement of the control objective.

It should be pointed out that the attack detection mechanism is based on the assumption that the attackers have no knowledge of the system being equipped with event-triggered controllers. In fact, most of the controllers are implemented to be successive with a determined sampling period in practice applications. Thus, this assumption is natural.

It is also worth noting that the proposed attack isolation method should keep the communication network connected after dropping the corrupted communication links. Thus, to protect the system from FDI attacks, the connectivity of the communication needs to be large enough. To this end, the following assumption needs to hold.

Assumption 1. The intact communication links, i.e., communication links which are not attacked, should maintain the connectivity of the communication network.

IV. Case Studies

In this section, the effectiveness of the proposed distributed event-triggered control scheme for frequency restoration of islanded MG is validated with a test MG, whose single-line diagram is illustrated in Fig. 4, in which 4 DGs and 2 loads are deployed. The inner control loops of primary control, including the voltage, current, and power control loops, are simulated in detail based on [9]. The time step of the test MG is set to be $1\times\ 10^{-6}$ s. The parameter settings are specified in Table I. The reference value of frequency for the secondary control of the islanded MG is set to be $\omega_{\rm ref} = 50$ Hz. From the communication topology of the test MG illustrated in Fig. 1, we can derive that $\delta_m = 3$, and the Laplacian matrix and the pinning matrix can be obtained as follows:

$$\boldsymbol{L} = \begin{bmatrix} 2 & -1 & 0 & -1 \\ -1 & 2 & -1 & 0 \\ 0 & -1 & 2 & -1 \\ -1 & 0 & -1 & 2 \end{bmatrix}, \ \boldsymbol{B} = \begin{bmatrix} 1 & 0 & 0 & 0 \\ 0 & 0 & 0 & 0 \\ 0 & 0 & 0 & 0 \\ 0 & 0 & 0 & 0 \end{bmatrix}$$

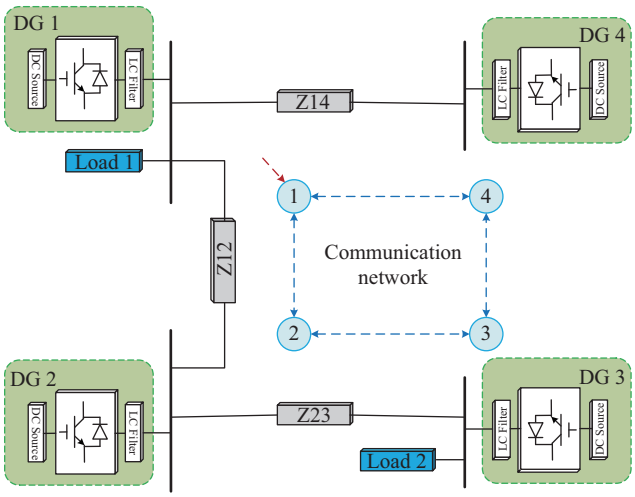

Fig. 4. The single-line diagram of the test MG.

TABLE I
Parameter Settings of The Test MG

Line	Line 1	R_{12}	0.12 Ω
		L_{12}	2.36 mH
	Line 2	R_{14}	0.1 Ω
		L_{14}	1.8 mH
	Line 3	R_{23}	0.12 Ω
		L_{23}	2.36 mH
DG	DG 1	P_{m1}	20 kW
		$K_1^{\rm P}$	1×10^{-5}
	DG 2	P_{m2}	10 kW
		$K_2^{\rm P}$	1×10^{-5}
	DG 3	P_{m3}	20 kW
		$K_3^{\rm P}$	5×10^{-5}
	DG 4	P_{m4}	10 kW
		$K_4^{\rm P}$	1×10^{-5}
Load	Load 1	P_1	35 kW
	Load 2	P_2	15 kW

$P_{{\rm m}i}$: the maximum active power output of DG i.

The parameter σ_i in the trigger condition is set to be 0.9. The control gain k is set to be 50, and the threshold is set to be $\gamma = 1 \times 10^{-3}$.

The effectiveness of the proposed event-triggered control scheme is validated with step load changes and FDI attacks on communication links.

A. Case 1: Performance of Step Response

The simulation process is set in the time sequence as follows:

1) At $t = 0$ s, the test MG is islanded from the main grid.
2) 0 s $< t <$ 1 s, the tested MG is governed only by the 5×10^6 primary control, and only Load 1 is connected.
3) At $t = 1$ s, the secondary control is started.
4) At $t = 2$ s, Load 2 is connected to the MG.
5) At $t = 3.5$ s, Load 2 becomes disconnected from the MG.

The total simulation time is set to be 5 s.

In Case 1, the performances of the proposed event-triggered controller with successive trigger condition checking (name it as Control Scheme 1 for conciseness) and the proposed event-triggered controller with reduced trigger condition checking (name it as Control Scheme 2 for conciseness) are evaluated and compared.

Figure 5 shows the simulation results of Control Scheme 1. It is observed that the frequency deviatess from 50 Hz after the MG islanding from the main grid, while the proposed control restores the frequency back to 50 Hz after starting and load changing. It is well worth noting that, dislike the traditional distributed secondary control, the curve of frequency is not smooth in the transient process due to the event-triggered mechanism. Fig. 6 shows the trigger time sequence of each DG. We can observe that the controller of each DG is triggered asynchronously and aperiodically according to its own trigger condition. The details of the trigger time sequence of DG 2 during 2 s to 3.5 s is illustrated in Fig. 7. It can be observed from Fig. 6, Fig. 7 and Table II that the communication requirements for each DG is significantly reduced during both the transient and steady states.

For Control Scheme 2, according to $\delta_m = 3$, $\sigma_i = 0.9$ and $k = 50$, one can derive from (29) that $h < 0.00033$. So, we choose $h = 0.0003$ to evaluate the trigger condition of Control Scheme 2. Figures 8–10 show the simulation results of Control Scheme 2. They exhibit a similar performance to that of its counterpart Control Scheme 1, which validates that

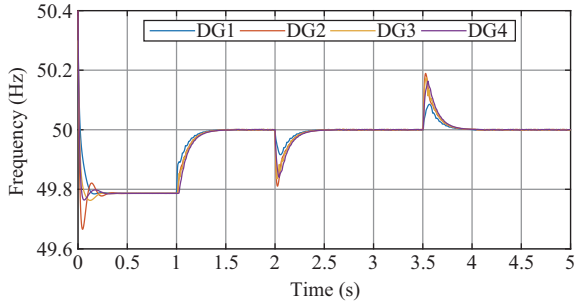

Fig. 5. The performance of Control Scheme 1 for Case 1.

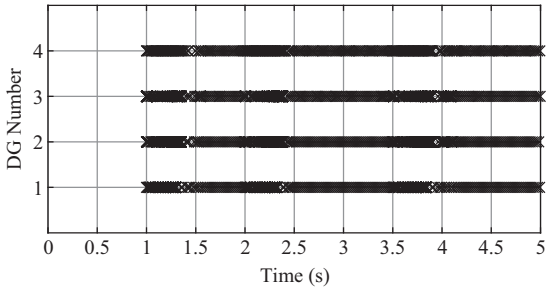

Fig. 6. The trigger time sequence of each DG of Control Scheme 1 in Case 1.

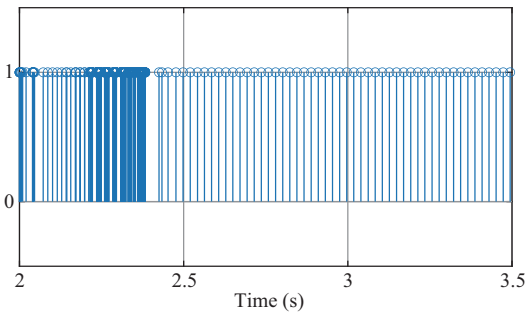

Fig. 7. The trigger time sequence of DG 2 of Control Scheme 1 during 2 s to 3.5 s.

TABLE II
TOTAL TRIGGER TIME OF EACH DG

Control Scheme	DG 1	DG 2	DG 3	DG 4
Control Scheme 1	490	1429	978	6148
Control Scheme 2	311	554	483	1104

*Each of DGs under traditional distributed control should trigger 5×10^6 times.

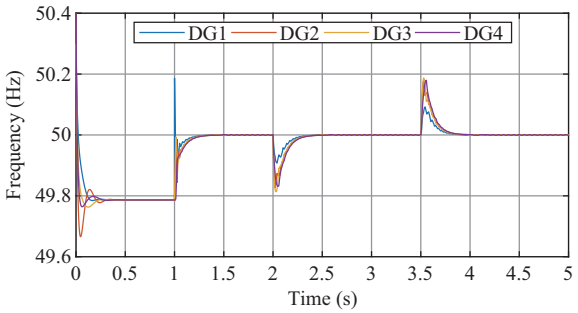

Fig. 8. The performance of Control Scheme 2 for Case 1.

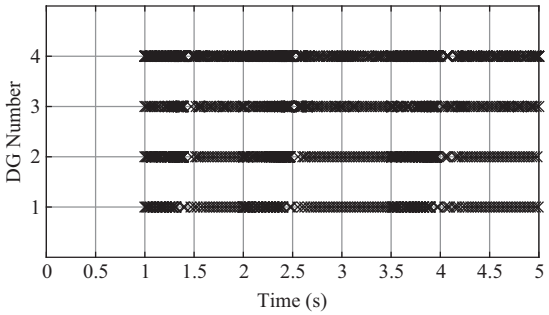

Fig. 9. The trigger time sequence of each DG of Control Scheme 2 in Case 1.

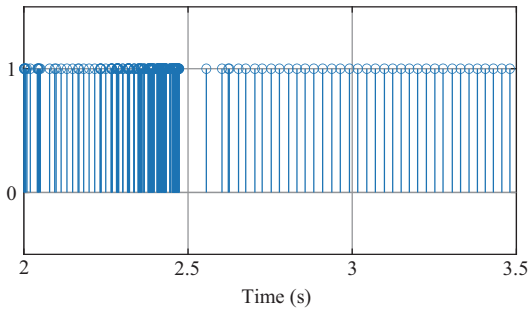

Fig. 10. The trigger time sequence of DG 2 of Control Scheme 2 during 2 s to 3.5 s.

the proposed event-triggered control scheme is effective for each DG checking the trigger condition with a longer period. However, we can also observe from Fig. 10 and Table II that Control Scheme 2 has better performance than Control Scheme 1 in the sense that each DG is triggered less under Control Scheme 2. The reason is that the DGs under Control Scheme 1 may trigger many times during the trigger condition checking period of Control Scheme 2 when $|e_i|$ and $|z_i|$ becomes very small. Consequently, the proposed event-triggered controller with reduced trigger condition checking can not only reduce the computation burden but also reduce more communication requirements than that of its counterpart.

B. Attack on Communication Link

Consider an unbounded attack $\Delta_{23} = 2t + \sin t$ injecting into the communication link between DG 2 and DG 3, which satisfies *Assumption 1*. The simulation process in the time sequence is set as:

1) At $t = 0$ s, the test MG becomes disconnected from the main grid.

2) 0 s $< t <$ 1 s, the tested MG is governed only by the primary control, and only Load 1 is connected.

3) At $t = 1$ s, the secondary control is started.

4) At $t = 2$ s, the attack is conducted.

The total simulation time is set to be 3 s.

Figure 11 illustrates the performance of the traditional secondary control under communication attack. It is observed that the conventional secondary control restores the frequencies back to 50 Hz, however, the frequencies of DGs are out of synchronous after the communication link between DG 2 and DG 3 being attacked, and the frequency stability is a failure. The performance of the event-triggered Control Scheme 2 with the attack detection principle described in Section III F is illustrated in Fig. 12. It can be noted that the event-triggered control with the attack detection principle can detect the corrupted communication link and turn it off immediately to protect the system, and the frequencies are restored back to 50 Hz after the isolation of attacks. The monitoring time is set to be 0.01 s, i.e., if any communication link transfers data successively with the sampling period of the control system (i.e., $1\mathrm{e}-6$) for 0.01 s, it is defined as being attacked. Fig. 13 shows the DT time sequence between DG 2 and DG 3 from the perspective of DG 3. The differences of DT between successive FDI attacks and normal communications are apparent, so DG 3 can easily determine that the information from DG 2 is corrupted, then DG3 shuts down its communication with DG 2 to isolate this attack.

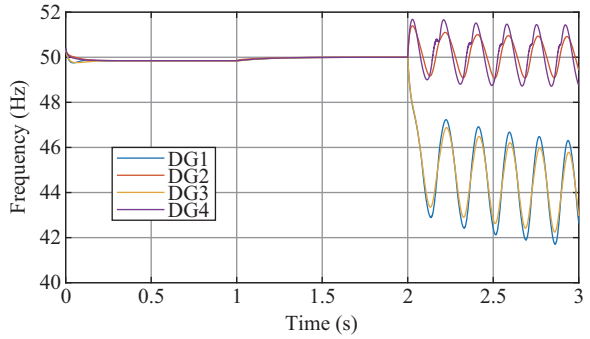

Fig. 11. The performance of the traditional secondary control under communication attack.

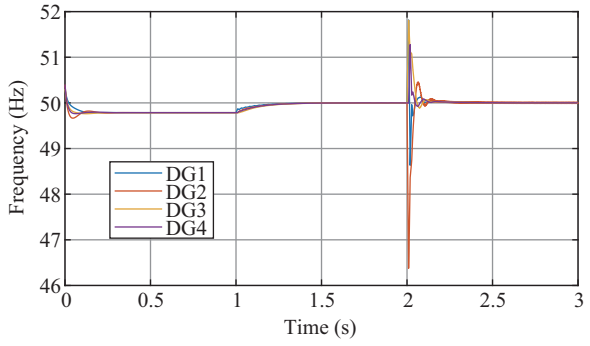

Fig. 12. The performance of the event-triggered secondary control with attack detection principle under communication attack.

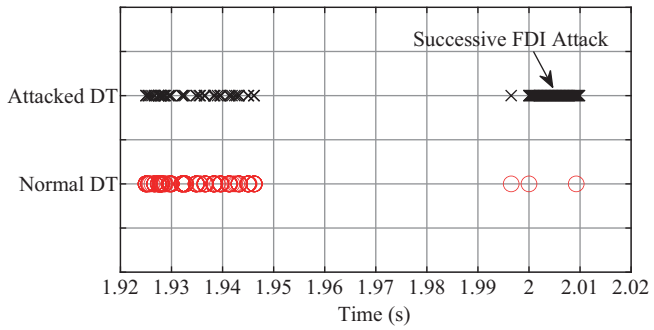

Fig. 13. The normal and attacked data transmission time sequence between DG 2 and DG 3.

V. Conclusion

In this paper, a distributed event-triggered control is proposed for the frequency restoration in islanded MGs. The event-triggered condition that evaluates when to trigger the controller is designed, and the Zeno behavior freeness is proved. To reduce the computation burden of each DG, a trigger condition checking period is derived. Each DG checks its trigger condition based on the selected period not only to significantly reduce the computation burden, but also to reduce more communication requirements. Furthermore, a simple attack detection and isolation method is proposed based on the property of communications. With the attack detection and isolation method, each DG can timely eliminate the successive FDI attack on communication links. The performances of the proposed control with step load changes and data corruption of communication links are evaluated by several simulation results, which verify that the designed event-triggered mechanism can significantly reduce the communication and computation requirements, and can protect the system against the attacks, thereby increasing the resilience of the system.

References

[1] Q. Zhou, M. Shahidehpour, A. Alabdulwahab, and A. Abusorrah, "A cyber-attack resilient distributed control strategy in islanded microgrids," *IEEE Transactions on Smart Grid*, vol. 11, no. 5, pp. 3690–3701, Sep. 2020.

[2] A. Nelson, S. Chakraborty, D. Wang, P. Singh, Q. Cui, L. Q. Yang, and S. Suryanarayanan, "Cyber-physical test platform for microgrids: combining hardware, hardware-in-the-loop, and network-simulator-in-the-loop," in *Proceedings of the 2016 IEEE Power and Energy Society General Meeting*, 2016, pp. 1–5.

[3] J. M. Guerrero, J. C. Vasquez, J. Matas, L. G. de Vicuna, and M. Castilla, "Hierarchical control of droop-controlled AC and DC microgrids—a general approach toward standardization," *IEEE Transactions on Industrial Electronics*, vol. 58, no. 1, pp. 158–172, Jan. 2011.

[4] A. Bidram and A. Davoudi, "Hierarchical structure of microgrids control system," *IEEE Transactions on Smart Grid*, vol. 3, no. 4, pp. 1963–1976, Dec. 2012.

[5] H. H. Xin, Z. H. Qu, J. Seuss, and A. Maknouninejad, "A self-organizing strategy for power flow control of photovoltaic generators in a distribution network," *IEEE Transactions on Power Systems*, vol. 26, no. 3, pp. 1462–1473, Aug. 2011.

[6] J. G. Zhou, S. Kim, H. G. Zhang, Q. Y. Sun, and R. K. Han, "Consensus-based distributed control for accurate reactive, harmonic, and imbalance power sharing in microgrids," *IEEE Transactions on Smart Grid*, vol. 9, no. 4, pp. 2453–2467, Jul. 2018.

[7] R. K. Han, L. X. Meng, G. Ferrari-Trecate, E. A. A. Coelho, J. C. Vasquez, and J. M. Guerrero, "Containment and consensus-based distributed coordination control to achieve bounded voltage and precise reactive power sharing in islanded AC microgrids," *IEEE Transactions on Industry Applications*, vol. 53, no. 6, pp. 5187–5199, Nov./Dec. 2017.

[8] Y. Wang, T. L. Nguyen, Y. Xu, Z. M. Li, Q. T. Tran, and R. Caire, "Cyber-physical design and implementation of distributed event-triggered secondary control in islanded microgrids," *IEEE Transactions on Industry Applications*, vol. 55, no. 6, pp. 5631–5642, Nov./Dec. 2019.

[9] A. Bidram, F. L. Lewis, and A. Davoudi, "Distributed control systems for small-scale power networks: using multiagent cooperative control theory," *IEEE Control Systems Magazine*, vol. 34, no. 6, pp. 56–77, Dec. 2014.

[10] A. Bidram, A. Davoudi, F. L. Lewis, and Z. H. Qu, "Secondary control of microgrids based on distributed cooperative control of multi-agent systems," *IET Generation, Transmission & Distribution*, vol. 7, no. 8, pp. 822–831, Aug. 2013.

[11] G. Y. Zhang, C. Y. Li, D. L. Qi, and H. H. Xin, "Distributed estimation and secondary control of autonomous microgrid," *IEEE Transactions on Power Systems*, vol. 32, no. 2, pp. 989–998, Mar. 2017.

[12] C. Deng and G. H. Yang, "Distributed adaptive fault-tolerant control approach to cooperative output regulation for linear multi-agent systems," *Automatica*, vol. 103, pp. 62–68, May 2019.

[13] R. F. Zhang and B. Hredzak, "Distributed finite-time multiagent control for DC microgrids with time delays," *IEEE Transactions on Smart Grid*, vol. 10, no. 3, pp. 2692–2701, May 2019.

[14] L. Ding, Q. L. Han, X. H. Ge, and X. M. Zhang, "An overview of recent advances in event-triggered consensus of multiagent systems," *IEEE Transactions on Cybernetics*, vol. 48, no. 4, pp. 1110–1123, Apr. 2018.

[15] D. V. Dimarogonas, E. Frazzoli, and K. H. Johansson, "Distributed event-triggered control for multi-agent systems," *IEEE Transactions on Automatic Control*, vol. 57, no. 5, pp. 1291–1297, May 2012.

[16] T. H. Cheng, Z. Kan, J. M. Shea, and W. E. Dixon, "Decentralized event-triggered control for leader-follower consensus," in *Proceedings of the 53rd IEEE Conference on Decision and Control*, 2014, pp. 1244–1249.

[17] C. Nowzari and J. Cortés, "Distributed event-triggered coordination for average consensus on weight-balanced digraphs," *Automatica*, vol. 68, pp. 237–244, Jun. 2016.

[18] B. Abdolmaleki, Q. Shafiee, A. R. Seifi, M. M. Arefi, and F. Blaabjerg, "A zeno-free event-triggered secondary control for AC microgrids," *IEEE Transactions on Smart Grid*, vol. 11, no. 3, pp. 1905–1916, May 2020.

[19] B. Abdolmaleki, Q. Shafiee, M. M. Arefi, and T. Dragičević, "An instantaneous event-triggered Hz-watt control for microgrids," *IEEE Transactions on Power Systems*, vol. 34, no. 5, pp. 3616–3625, Sep. 2019.

[20] Z. J. Lian, C. Deng, C. Y. Wen, F. H. Guo, P. F. Lin, and W. T. Jiang, "Distributed event-triggered control for frequency restoration and active power allocation in microgrids with varying communication time delays," *IEEE Transactions on Industrial Electronics*, vol. 68, no. 9, pp. 8367–8378, Sep. 2021.

[21] D. Pullaguram, S. Mishra, and N. Senroy, "Event-triggered communication based distributed control scheme for DC microgrid," *IEEE Transactions on Power Systems*, vol. 33, no. 5 pp. 5583–5593, Sep. 2018.

[22] J. Zhang, X. Wang and L. Ma, "A Finite-time Distributed Cooperative Control Approach for Microgrids," *CSEE Journal of Power and Energy Systems*, vol. 8, no. 4, pp. 1194–1206, Jul. 2022.

[23] C. Godsil and G. Royle, *Algebraic Graph Theory*, New York: Springer, 2001.

[24] X. Wang, J. Zhang, M. Zheng and L. Ma, "A distributed reactive power sharing approach in microgrids with improved droop control," *CSEE Journal of Power and Energy Systems*, vol. 7, no. 6, pp. 1238–1246, Nov. 2021

[25] P. Barooah and J. P. Hespanha, "Graph effective resistance and distributed control: spectral properties and applications," in *Proceedings of the 45th IEEE Conference on Decision and Control*, 2006, pp. 3479–3485.

[26] N. A. Lynch, *Distributed Algorithms*, San Francisco: Morgan Kaufmann, 1997.

[27] W. Ren and R. W. Beard, *Distributed Consensus in Multi-vehicle Cooperative Control: Theory and Applications*, London: Springer, 2008.

[28] C. Y. Li, Z. H. Qu, D. L. Qi, and F. Wang, "Distributed finite-time estimation of the bounds on algebraic connectivity for directed graphs", *Automatica*, vol. 107, pp. 289–295, Sep. 2019.

[29] S. Abhinav, H. Modares, F. L. Lewis, F. Ferrese, and A. Davoudi, "Synchrony in networked microgrids under attacks," *IEEE Transactions on Smart Grid*, vol. 9, no. 6, pp. 6731–6741, Nov. 2018.

Yulin Chen received the Ph.D. degree in Electrical Engineering from Zhejiang University, Hangzhou, China, in 2021. He was a Postdoctoral Fellow with University of Macau, Macau, China, from September 2021 to September 2022. He is currently an Associate Research Fellow with Hainan Institute of Zhejiang University, Sanya, China. His current research interests include distributed control of renewable energy and cyber-physical security with application in smart grid.

Donglian Qi received her Ph.D. degree in Control Theory and Control Engineering from Zhejiang University, Hangzhou, China, in March 2002. Since then, she has been with the College of Electrical Engineering, Zhejiang University where she is currently a Professor. Her current research interests include the basic theory and application of cyber physical power system (CPPS), digital image processing, artificial intelligence, and electric operation and maintenance robots. She is an Editor for the Clean Energy, the IET Energy Conversion and Economics, and the Journal of Robotics, Networking and Artificial Life.

Zhenming Li received her B.Eng. and Ph.D. degrees at Zhejiang University, Hangzhou, China, in 2017 and 2022, respectively. She was a Research Assistant at Hong Kong Polytechnic University (PolyU) (2021–2022), Hong Kong, China. Her current research interests include voltage optimization and control of renewable energy and cyber-physical security in smart grids.

Zhenyu Wang received the Bachelor's degree in Network Engineering from Hainan University, Haikou, China, in June 2014, and the Master's degree in Electronic and Communication Engineering from Jiangnan University, Wuxi, China, in June 2017. He is currently pursuing the Ph.D. degree with the College of Electrical Engineering, Zhejiang University, Hangzhou, China. His current research interests include intelligent perception of power system and cyber-physical security with application in smart grid.

Xinyi Yang received the Bachelor's degree in Atmospheric Science from Nanjing University of Information Science and Technology University, Nanjing, China, in June 2016, and the Master's degree in Meteorology from Zhejiang University, Hangzhou, China, in June 2019. She is currently pursuing the Ph.E. degree with the College of Electrical Engineering, Zhejiang University, Hangzhou, China. Her current research interests include renewable energy planning, forecasting and risk management.

Jianliang Zhang received his Ph.D. degree in Control Theory and Control Engineering from Zhejiang University, Hangzhou, China, in June 2014. Since then, he has been working with College of Electrical Engineering, Zhejiang University (ZJU). He was a visiting scholar at Hong Kong Polytechnic University (PolyU) (2016–2017), Hong Kong, China. His current research interests include distributed optimization, with applications to energy/power systems, and cyber-physical security with applications in smart grids.